Study on the Formability & Shape Conformity of Mg & Al-alloy sheets in Warm condition by Electromagnetic Forming

M. Singhal, P. P. Date
IIT Bombay, India

5th International Conference on High Speed Forming
24th – 26th April, Dortmund, Germany

OUTLINE

- Introduction
- Background
- Current Work - Simulation Plan
- Configuration & Numerical Model
- Material Model
- Failure Criteria Based on Strain Distribution
- Results & Discussions
- Conclusions

MAGNESIUM

- Lightest Structural Material
- Great Potential of Mass Saving compared to Al

BUT Difficult to form at Room Temperature with conventional forming methods

	Al	Mg	Steel	Ti
ρ	2.8	1.74	7.83	4.5
E	70	45	210	110
R_m	150-680	100-380	300-1200	910-1190
$R_m/\rho^{(1)}$	54-243	57-218	38-153	202-264
$E/\rho^{(2)}$	25.0	25.9	26.8	24.4
$\sqrt{R_m}/\rho^{(3)}$	9.3	11.2	4.4	7.7
$\sqrt[3]{E}/\rho^{(4)}$	14.7	20.4	7.6	10.6

ρ Density [kg dm^{-3}], E Tensile modulus [GPa],
R_m Tensile strength [N mm^{-2}]
(1) Specific strength [10^6 N mm kg^{-1}]
(2) Specific stiffness [10^9 N mm kg^{-1}]
(3) Dent resistance [10^6 N$^{1/2}$ mm^2 kg^{-1}]
(4) Shell stiffness [10^7 N$^{1/3}$ mm$^{7/3}$ kg^{-1}]

Comparison of Metals in terms of their Properties. [Kleiner et.al., 2003]

INTRODUCTION

	Steel parts (kg)	Mg parts (kg)	Weight saving (kg)
CHASSIS			
1A frame cross member	9.1	4.6	4.5
Fuel tank barrier	4.0	2.3	1.7
Brackets-adjustable pedal	0.9	0.50	0.4
Brake/accelerator	1.1	0.90	0.2
Steering-column brackets	0.9	0.70	0.2
INTERIOR			
Seats–frames [4]	20	7.3	13
Stanchions [2]	11	5.9	5.0
IP-X-car beam	11	6.8	4.6
Knee bolster	4.6	2.7	1.9
Console	3.6	2.3	1.3
Brackets	0.50	0.20	0.30
Glove box door	0.50	0.30	0.20
BODY STRUCTURE			
Door inner panels [4]	39	18	21
Radiator support/GOR	15	5.5	9.0
Front of dash structure	18	10	8.2
Lift gate inner	10	5.5	4.5
Windshield surround (frame)	10	5.5	4.5
Targa roof frame opening	5.0	2.7	2.3
Headlight retainer	0.70	0.50	0.20
TOTAL	165	82	83

Potential steel parts in automotives which can be replaced of by Mg parts

[Du et. al., 2009]

50% Weight Reduction

INTRODUCTION

- **Forming at HIGH TEMPERATURE:**
  - Dynamic Recovery (DRV)
  - Dynamic Recrystallization (DRX)
  - Activation of non-basal slip system

- **Forming at HIGH STRAIN RATE:**

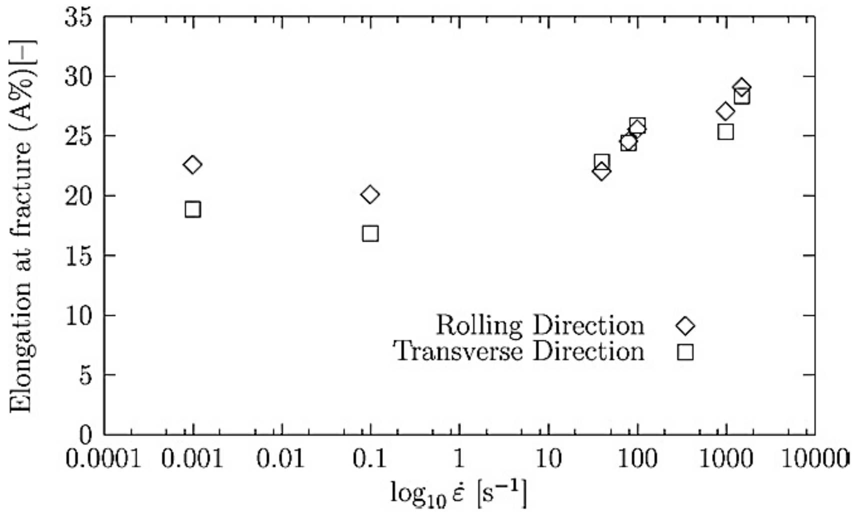

Elongation at fracture at room temperature for different strain rates [Ulacia et.al., 2010]

INTRODUCTION

- **EMF - High Velocity, Non-Contact forming technique, in which large forces can be imparted to a conductive metallic work piece by pure electromagnetic interactions.**
- **Applications**
  - Sheet metal Forming
  - Tube forming

BACKGROUND

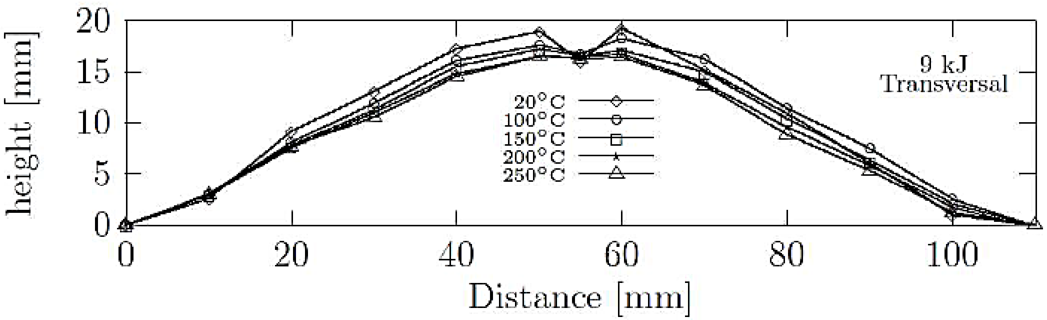

Ulacia et. al., 2010

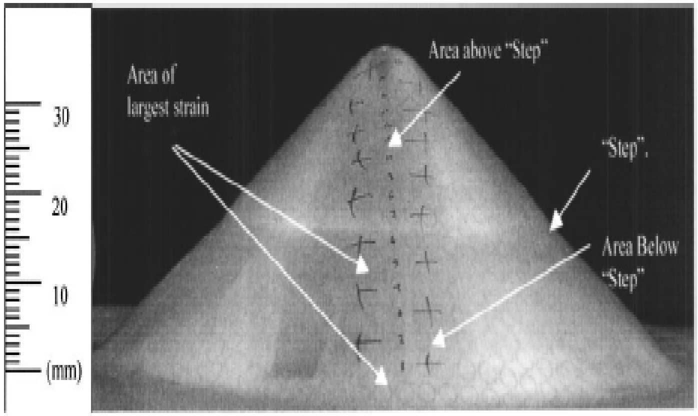

- **Increased Formability of AZ31B at warm working conditions**
- **Inconsistency of FLD based criteria to predict formability**
- **New parameters to characterize Mechanical Behavior**

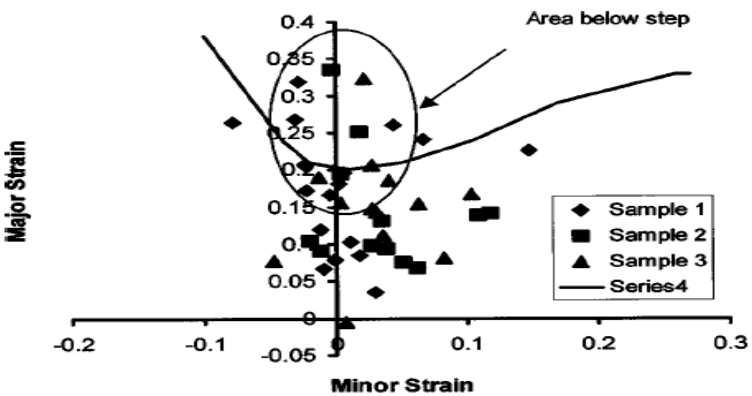

Imbert et. al., 2004

CURRENT WORK - SIMULATION PLAN

Factor	Level 1	Level 2
Sheet End Constraint	Fully Unclamped (FF)	Fully Clamped (FC)
Material	Mg alloy (AZ31B-H24)	Al alloy (AA2024-T4)
Energy Levels	4.3 kJ	8.2 kJ
Initial temp. of sheet	423K	523K

- **16 (2^4) Simulations with Full Factorial Design Approach**
- **Output Parameters:**
  - Strain Non-uniformity Index (SNI) [Lower the better] [Date et. al., 2006]
  - Maximum filled groove height/Total groove height (H_F/H_T x 100) [Higher the better]
- **ANOM approach used to analyze the simulated results**
- **AIM- Maximum Cavity filling without Severe Thinning**

FULL-FACTORIAL DESIGN

Run	Sheet End Constraint	Material	Energy Level (kJ)	Initial temp. of sheet (K)	SNI	H_F/H_T X 100
1	FF	AZ31B	4.3	423	0.0156	34.64534
2	FF	AZ31B	4.3	523	0.0167	36.37234
3	FF	AZ31B	8.2	423	0.0299	43.20681
4	FF	AZ31B	8.2	523	0.0378	46.11756
5	FF	AA2024	4.3	423	0.0106	36.90238
6	FF	AA2024	4.3	523	0.0145	36.93281
7	FF	AA2024	8.2	423	0.0229	50.49213
8	FF	AA2024	8.2	523	0.0278	54.56981
9	FC	AZ31B	4.3	423	0.0129	29.25869
10	FC	AZ31B	4.3	523	0.0151	33.10647
11	FC	AZ31B	8.2	423	0.0259	35.53459
12	FC	AZ31B	8.2	523	0.0298	39.58488
13	FC	AA2024	4.3	423	0.0110	31.75159
14	FC	AA2024	4.3	523	0.0132	32.97294
15	FC	AA2024	8.2	423	0.0194	42.00009
16	FC	AA2024	8.2	523	0.0215	47.23350

CONFIGURATION

- **3D Geometry realized as 2D-Axisymmetric**
- **Virtual Circuit generated is connected to the coil via Terminals**
- **Sheet Thickness = 1 mm**

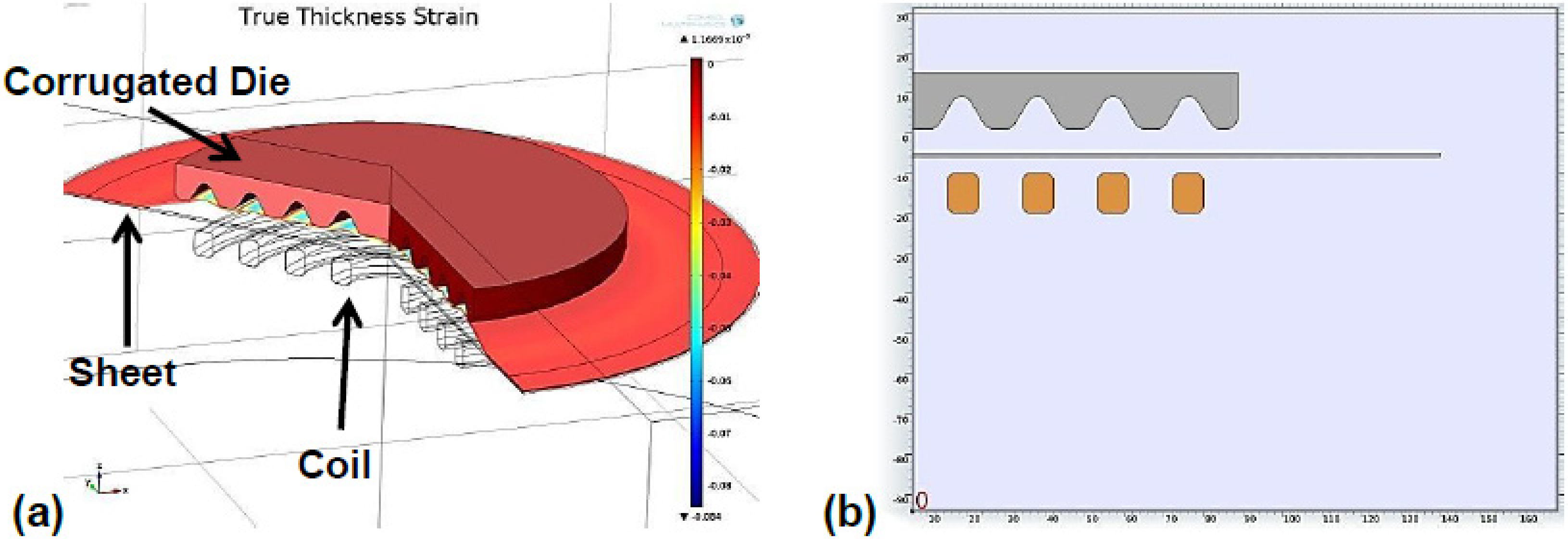

(a) 3D Configuration, (b) 2D axisymmetric configuration

NUMERICAL MODEL

FULLY COUPLED PHYSICS

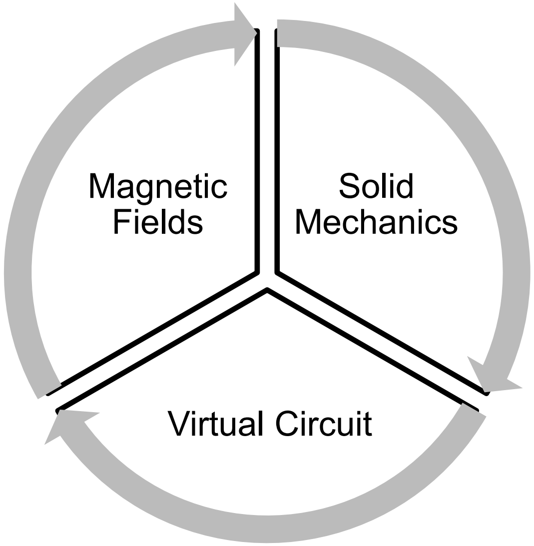

- Virtual Circuit
  - Considering each turn of the coil as a separate domain and connecting them via. Virtual Terminals
  - A Capacitor with defined initial Voltage
  - Total Resistance of the circuit
  - Applying KVL & solving taking Laplace to get the real-time current values
- Magnetic Fields
  - Taking Currents from Virtual Circuit as input & solves for strong Transient Magnetic field using Maxwell's equations
  - Solves for Induced Current density & Magnetic forces generated
- Solid Mechanics
  - Takes Maxwell stress tensor as input for body loads & Calculates the amount of deformation.
  - Accounts for thermal strains

NUMERICAL MODEL

- Penalty Factor Method used for Contacts
- Static Coulomb Friction Model
- Rayleigh Damping Model
  - Mass & stiffness Damping
- Dynamic-Transient Model

MATERIAL MODEL

Modified Johnson-Cook model with the Cowper-Symonds formulation for Mg AZ31B-H24

$$\sigma = \left(A + B\varepsilon_p^n\right)\left[1 + \left[\frac{\dot{\varepsilon}}{C}\right]^{\frac{1}{p}}\right]\left[1 - \left(\frac{T - T_R}{T_M - T_R}\right)^m\right] \qquad (1)$$

Parameter in CS model for Mg AZ31B-H24 for rolling direction [Hasenpouth, 2010]

Parameter	Estimate	Lower 95%	Upper 95%
A [MPa]	202.768	190.136	215.400
B [MPa]	180.932	171.468	190.396
n	0.229	0.193	0.265
C [1/s]	5e4	-	-
p	2.157	2.109	2.205
m	1.393	1.380	1.406

MATERIAL MODEL

Johnson-Cook model for AA2024-T4

$$\sigma = \left(A + B\varepsilon_p^n\right)\left[1 + C\left[\frac{\dot{\varepsilon}}{\dot{\varepsilon}_0}\right]\right]\left[1 - \left(\frac{T - T_R}{T_M - T_R}\right)^m\right] \qquad (2)$$

Parameters in JC model for AA2024-T4 [Lee et.al., 2010]

A [MPa]	B [MPa]	N	C	m	$\dot{\varepsilon}_0[s^{-1}]$	$T_R[K]$	$T_M[K]$
390	1980	0.4890	0.0140	0.6	0.0001	298	775

FAILURE CRITERIA

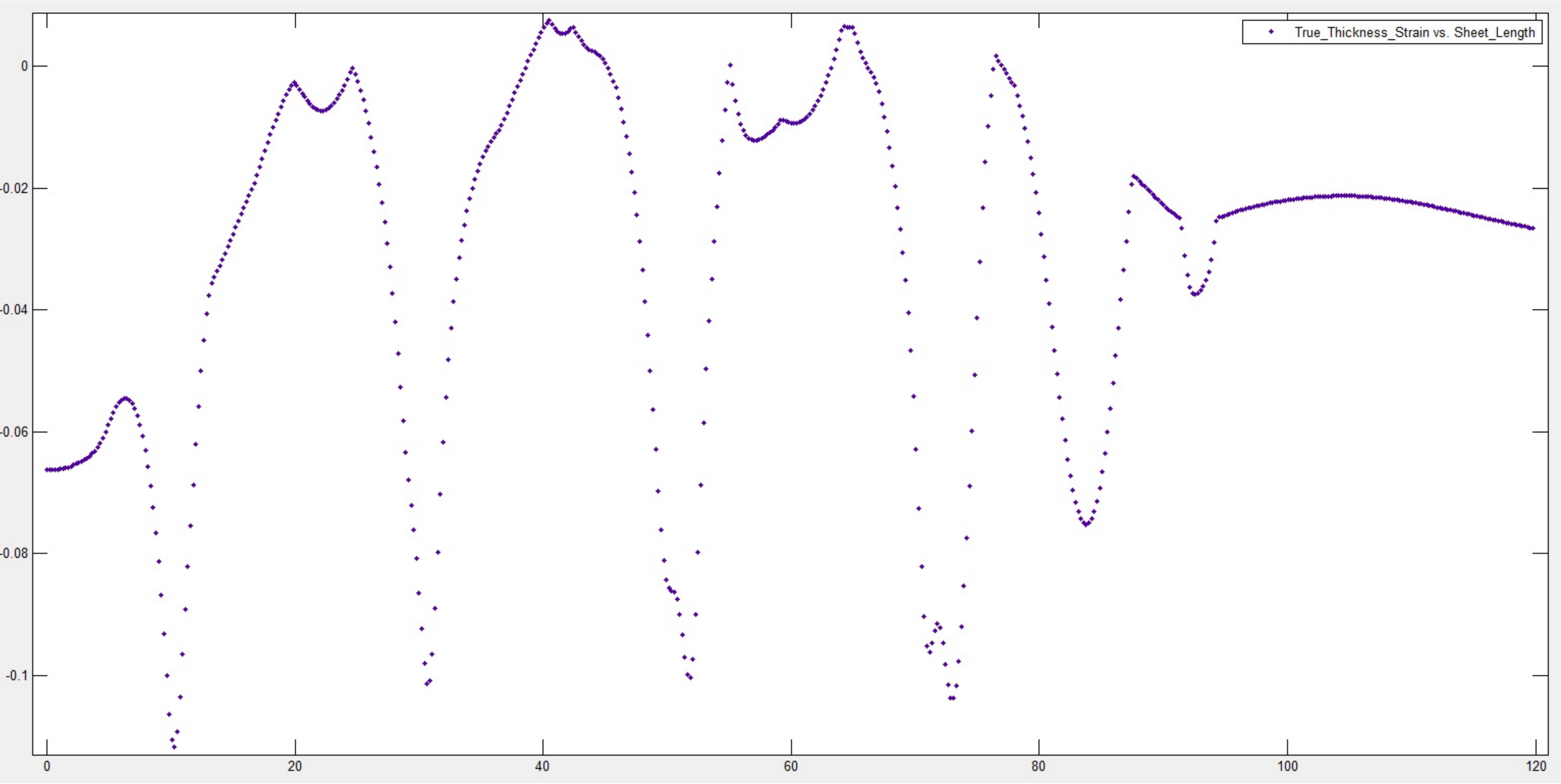

FAILURE CRITERIA

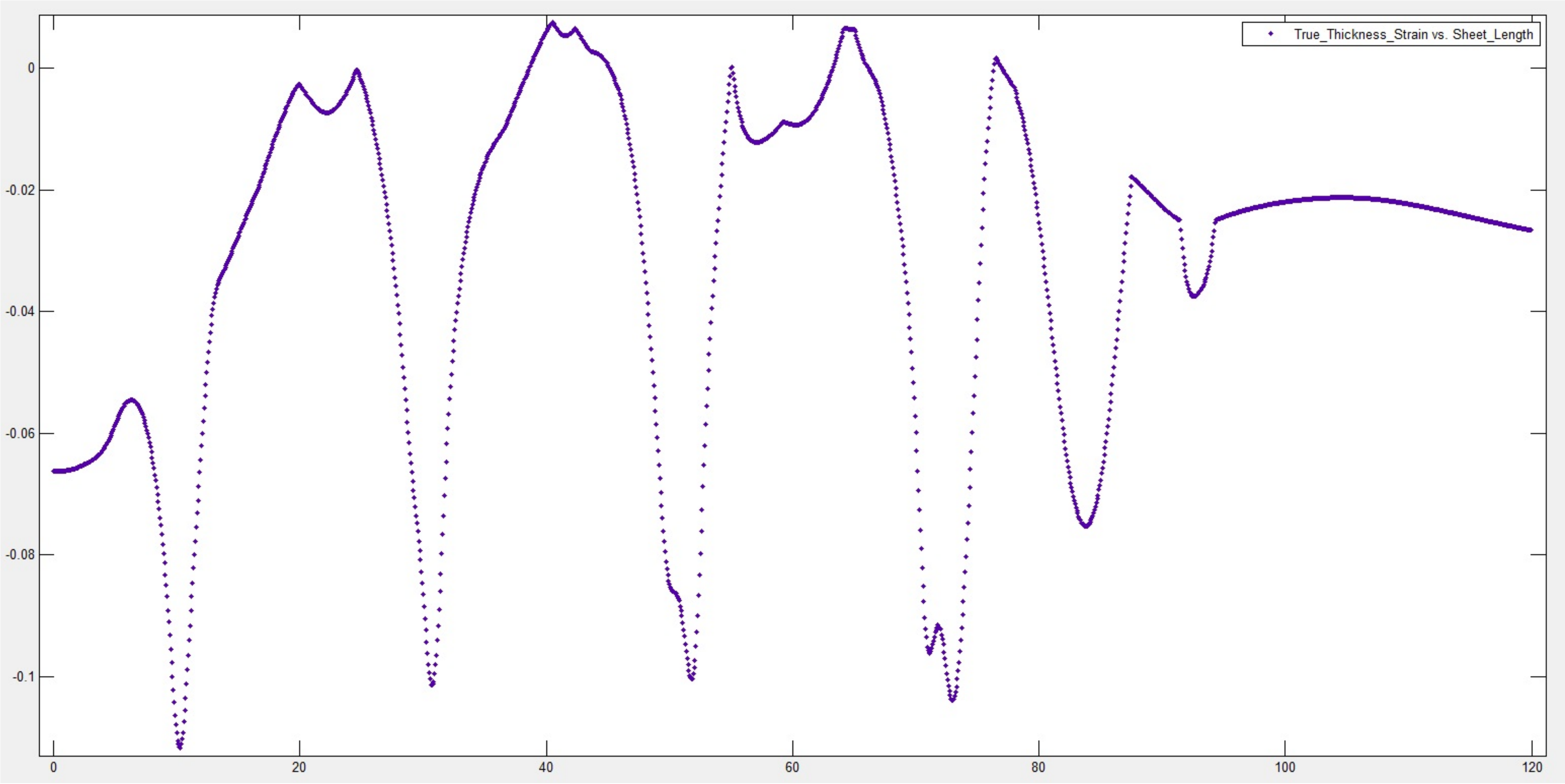

FAILURE CRITERIA

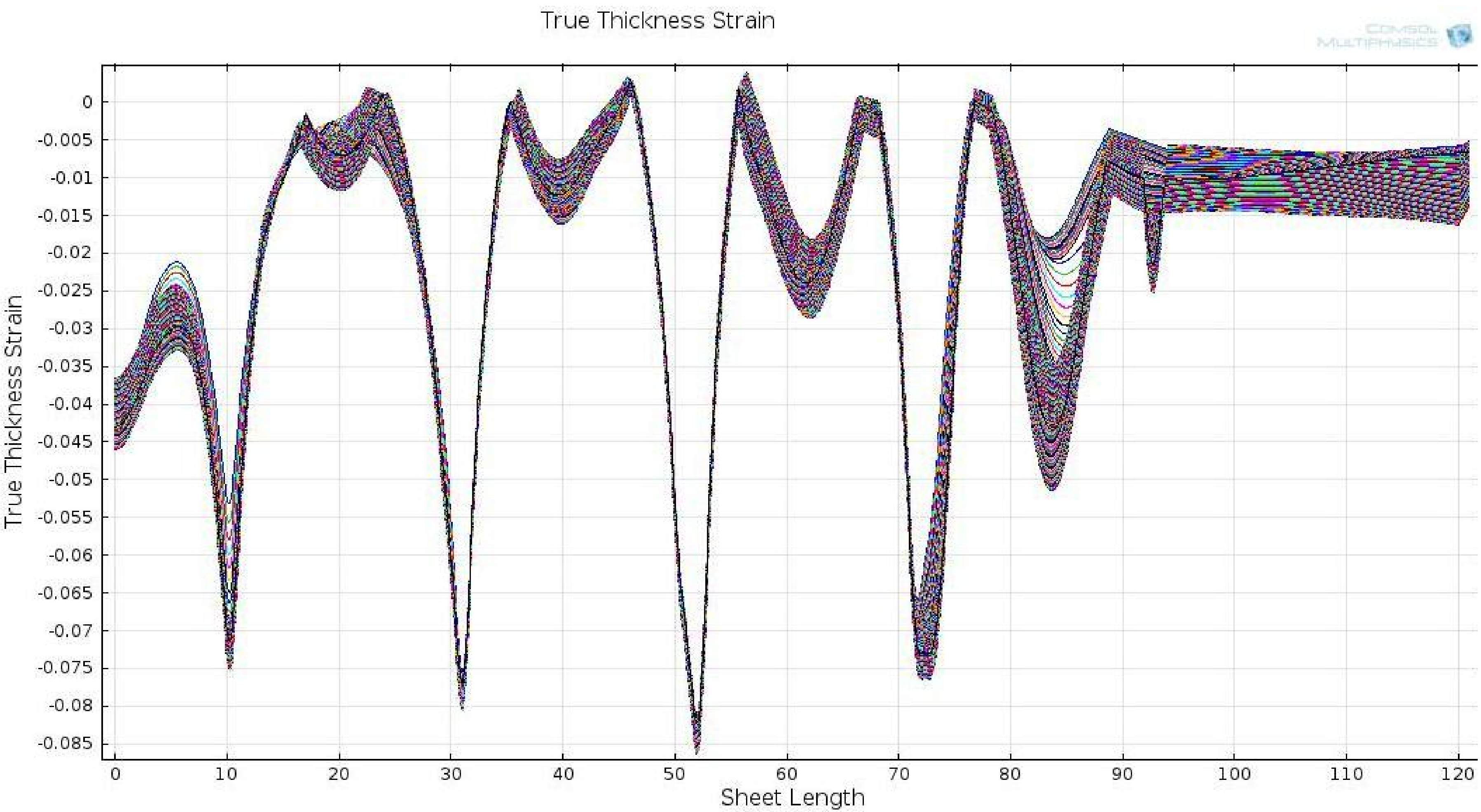

Failure criteria based on strain distribution

- Strain Distribution data is plotted on the plane
- Fitted to the Fourier Series of High order (850 in the present case)*
- Curvature(K) of the strain peaks is captured with high precision#

* **R-squared** value near about **0.9970**

\# **Central Differentiation technique with 8th order accuracy**

$$K = \left(\frac{d^2\varepsilon}{dx^2}\right) \Big/ \left[1 + \left(\frac{d\varepsilon}{dx}\right)^2\right]^{3/2} \quad (3)$$

$$\frac{d^2\varepsilon}{dx^2} = SNI + \sum_{n=1}^{m} -\left[1 + \left(\frac{n\pi}{L}\right)^2\right]\left[a_n cos\left(\frac{n\pi x}{L}\right) + b_n sin\left(\frac{n\pi x}{L}\right)\right] \quad (4)$$

RESULTS & DISCUSSIONS

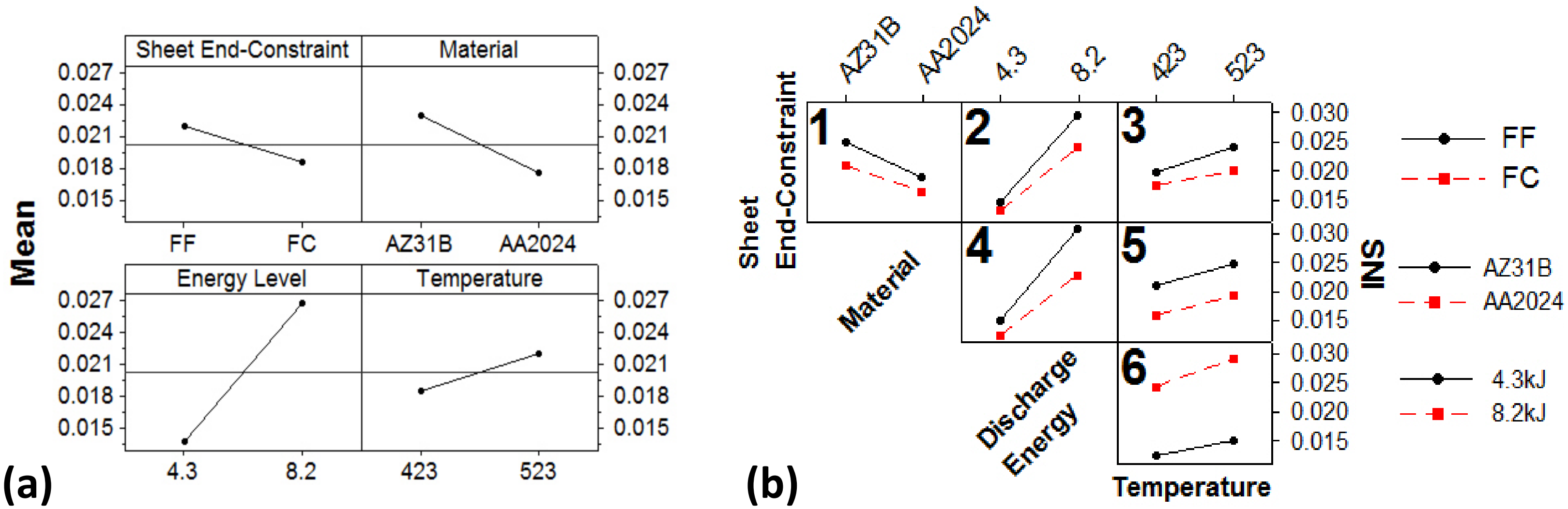

(a) Main effect plots, (b) Interaction plots, of all the factors taking SNI as a response.

- **Higher SNI value for Mg-alloy for both end-constraint conditions.**
- **Clamping conditions influences more at higher discharge energies.**
- **Effect of temperature on SNI is pronounced when using the high discharge energy**
- **low discharge energy, fully constrained condition and a low temperature favours a low SNI.**

RESULTS & DISCUSSIONS

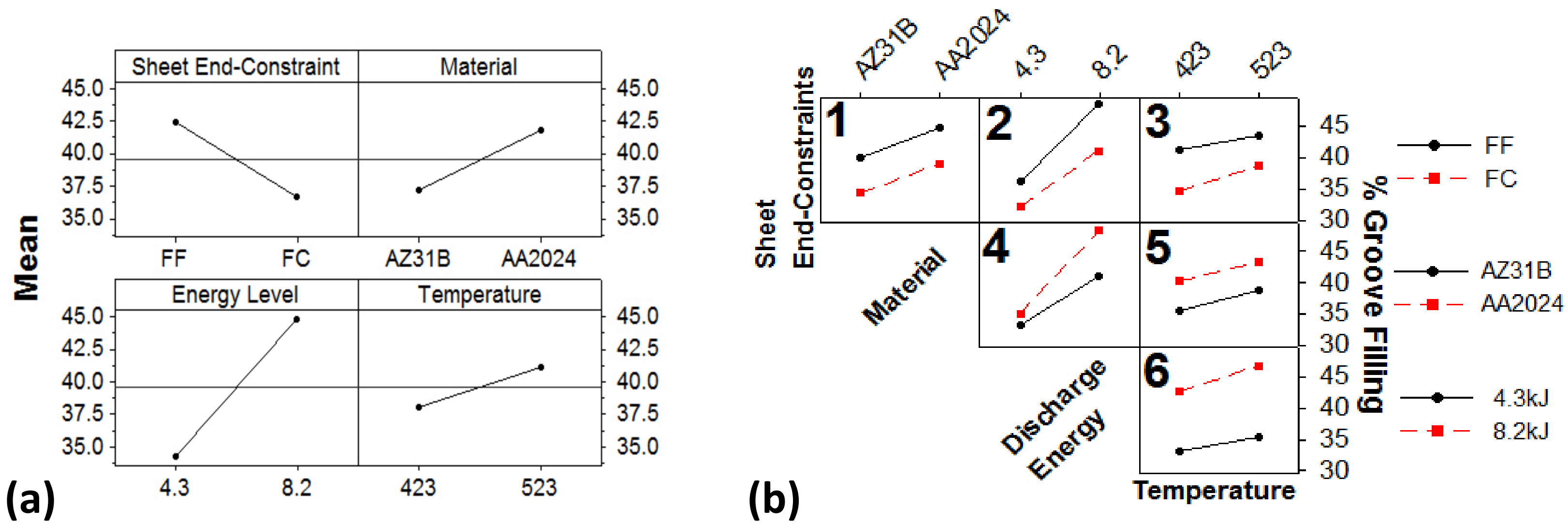

(a) Main effect plots, (b) Interaction plots, of all the factors taking maximum filled groove height/Total groove height as a response.

- **Filling is better with an unclamped condition.**
- **Equally sensitive to the status of clamping in case of the two materials.**
- **With increasing discharge energy, increase in cavity filling is more rapid for an unclamped condition**
- **Die filling is more sensitive to temperature when the sheet is fully clamped**
- **Sensitivity of die filling to temperature increases with an increase in discharge energy**
- **High discharge energy, unclamped condition and high temperature results in better die filling.**

RESULTS & DISCUSSIONS

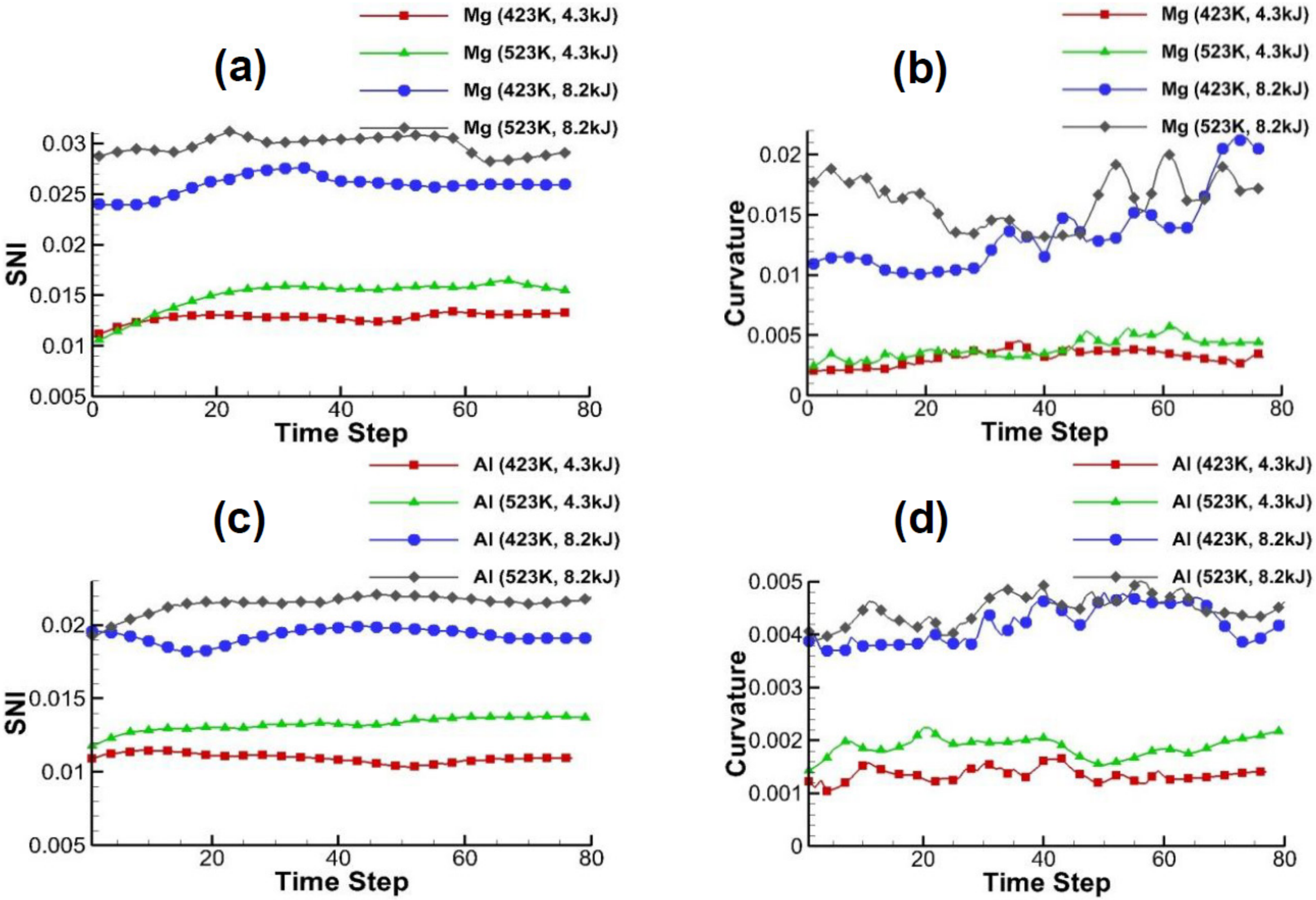

(a) & (c) SNI plots, (b) & (d) Curvature plots for runs with Mg-alloy & Al-alloy respectively for fully Clamped end condition.

CONCLUSIONS

- Favourable conditions for die filling and a more uniform strain distribution counter each other.
- Optimum conditions permitting some degree of drawing in, together with optimal discharge energy could be established at a given temperature of forming to facilitate rapid die filling at a low SNI.
- Regulated blank holding force could be a better alternative.

CONCLUSIONS

- Effect of temperature becomes more & more significant if the value of discharge energy is near upper limit used to form a sample without failure.
- The critical value of SNI and curvature may be verified experimentally.

Thank You for your attention